

A systematic DFT screening of cationic faujasite-type zeolites for the adsorption of NO, NO₂ and H₂O

Electronic Supplementary Information

Ioannis Karamanis^{a,b}, Ayoub Daouli^b, Hubert Monnier^a, Marie-Antoinette Dziurla^c, Guillaume Maurin^d, Michael Badawi^{b,c*}

^a Institut National de Recherche et de Sécurité, 1 Rue du Morvan, CS60027, 54519 Vandœuvre-lès-Nancy Cedex, France

^b Laboratoire de Physique et Chimie Théoriques, UMR CNRS 7019, Université de Lorraine, F-54000, Nancy, France

^c IUT de Moselle-Est, Université de Lorraine, Saint-Avold, France.

^d ICGM, Université de Montpellier, CNRS, ENSCM, Montpellier, France.

*Corresponding author: michael.badawi@univ-lorraine.fr

Table SI: Parameters of the cells used. The matrix of the cell parameters is 3X3 as seen below.

Cell	axis	X	Y	Z
LiY	X	17.48279984	0.028468534	-0.010319501
	Y	8.840644478	15.10530102	0.001263263
	Z	8.953000395	5.186455266	14.30151694
NaY	X	17.83194901	-1.22E-04	-0.028527718
	Y	8.891369642	15.20535001	-0.012376228
	Z	9.008870912	5.331352808	14.47801799

KY	X	17.88242991	0.013399027	-0.022310091
	Y	8.969844509	15.21942585	-0.006752499
	Z	9.046752553	5.32724579	14.54203205
RbY	X	17.8220724	0.017842701	-0.028852805
	Y	8.872341967	15.25630517	-0.016960456
	Z	9.019747107	5.323323404	14.46825396
CsY	X	17.79319373	0.026282437	-0.030084551
	Y	8.847363736	15.23561722	-0.016684936
	Z	9.012119865	5.319173337	14.44479319
CuIY	X	17.69461509	0.005533381	-0.015061614
	Y	8.906587859	15.17316108	-0.00268668
	Z	8.949985666	5.22394246	14.37118436
AgY	X	17.82524546	0.023009813	-0.028088024
	Y	8.880991429	15.32137819	0.005711805
	Z	8.958022677	5.31230187	14.54800329
CaY	X	17.56170831	0.131723813	0.103303089
	Y	8.878751494	15.34634733	0.003723999
	Z	8.891002006	5.141876132	14.47215009
BaY	X	17.65739619	0.197592615	0.157008324
	Y	8.983397819	15.558916	0.022902052
	Z	9.001210744	5.22787995	14.55107451
ZnY	X	17.4541068	0.122307802	0.222089139
	Y	8.815425302	15.13138704	0.158866791
	Z	8.931016264	5.157649615	14.44206101
CuIIY	X	17.30853447	0.144358639	0.312544215
	Y	8.760911454	15.11543416	0.166930556
	Z	8.936631394	5.120753288	14.46748513

PdY	X	17.62329264	0.230506831	0.10947841
	Y	8.994678643	15.35556634	0.049814261
	Z	8.954558123	5.218480772	14.53710812
PtY	X	17.53141983	0.291843634	0.070306227
	Y	8.999833178	15.40006848	0.01764803
	Z	8.893854019	5.24300261	14.48522903
FeY	X	17.50640945	0.390115192	0.205316363
	Y	9.073682875	15.44158663	0.063068069
	Z	9.021402311	5.267918167	14.34289535
CoY	X	17.58637875	0.294444132	0.14215959
	Y	9.032084866	15.29525744	0.106447387
	Z	8.981756115	5.257715159	14.41576421
NiY	X	17.3893343	0.293164911	0.141810096
	Y	8.933382807	15.18903178	0.151598882
	Z	8.882548702	5.264660529	14.55657155
LiX	X	17.20779103	-0.099117749	-0.033554342
	Y	8.338860954	15.21910813	-0.067090683
	Z	8.313796344	4.775980281	14.42869594
NaX	X	17.50382636	-0.131349582	0.0169997
	Y	8.455522484	15.37393218	0.051261406
	Z	8.490991148	4.903275144	14.71353001
KX	X	17.86417227	0.102227913	0.085683286
	Y	8.836784935	15.54315865	0.17768206
	Z	8.789938477	5.123316737	14.81413347
RbX	X	17.76150318	-0.067543852	0.020097229
	Y	8.842103836	15.48536092	-0.102119503
	Z	8.868095283	5.141645087	14.61398294

CsX	X	17.50088428	0.345714795	0.220266252
	Y	8.082573939	15.56428608	0.212631853
	Z	8.054974766	4.932908444	14.77715554
CuIX	X	17.62051503	-0.010132539	0.114160925
	Y	8.617120596	15.29570477	0.107523483
	Z	8.662434278	4.927601359	14.64341397
AgX	X	17.81225847	0.054675081	0.009557503
	Y	8.758736933	15.47997897	0.009327313
	Z	8.789320613	5.027229698	14.70153928
CaX	X	17.61194975	0.263403809	0.371209908
	Y	8.624573607	15.46104291	0.20133009
	Z	8.909050686	5.125985862	14.85135332
CuIIIX	X	17.67742153	0.177255785	0.353225077
	Y	8.579003098	15.52226593	0.264419036
	Z	8.899130319	5.185531733	14.38814033
PdX	X	17.83957706	0.249977681	0.180537079
	Y	8.719619091	15.56567803	0.032198283
	Z	8.853928903	5.080695317	14.48579026
PtX	X	17.825907	0.184276319	0.170238245
	Y	8.656290352	15.45583077	0.082535494
	Z	8.820879476	5.076330333	14.51127437
FeX	X	17.78957072	0.185862305	0.002613992
	Y	8.639262577	15.43725461	0.030610093
	Z	8.661412834	5.097080758	14.42098654
CoX	X	17.57506741	0.280839684	0.089658921
	Y	8.621063543	15.4326837	0.017277895
	Z	8.65751587	5.074782613	14.30456417

NiX	X	17.72344761	0.234706778	-0.236718482
	Y	8.651499869	15.66373621	-0.104939962
	Z	8.442070368	5.164781487	14.17715624

Table SII: Stretching induced to the intramolecular bonds of the gases during the adsorptions over the different Y and X cation-exchanged faujasites.

Gas species concerned	NO			H ₂ O	
Bond	N-O	O1-NO	O2-NO	H1-OH	H2-OH
Initial length (Å)	1.17	1.21	1.21	0.97	0.97
LiY	0.00	-0.01	0.01	0.00	0.01
NaY	0.00	0.02	-0.01	0.01	0.00
KY	0.00	0.01	0.01	0.02	0.00
RbY	0.00	0.01	0.01	0.01	0.01
CsY	0.00	0.01	0.01	0.01	0.01
Cu(I)Y	0.02 (2%)	0.08 (7%)	0.02 (2%)	0.03 (3%)	0.00 (0%)
AgY	0.00	0.01	0.01	0.00	0.02
CaY	-0.01	0.05	0.00	0.00	0.01
BaY	0.00	0.02	0.03	0.02	0.02
ZnY	0.00	0.06	0.00	0.01	0.00
Cu(II)Y	-0.02	0.02	-0.01	0.01	0.03
PdY	-0.01	0.00	0.00	0.01	0.01
PtY	0.00	0.00	0.01	0.01	0.01

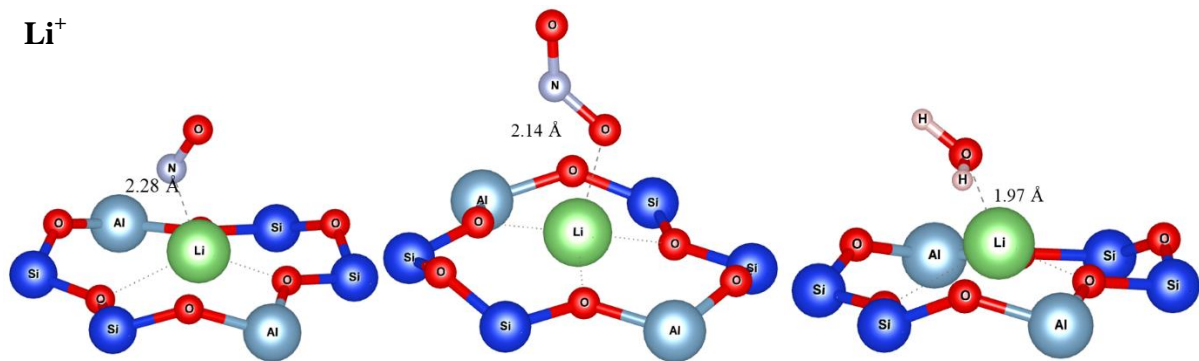
FeY	0.00 (0%)	-0.04 (3%)	0.31 (26%)	0.00 (0%)	0.01 (1%)
CoY	-0.01	-0.05	0.35	0.02	0.01
NiY	-0.01	0.03	-0.01	0.01	0.01
LiX	-0.01	0.02	0.02	0.02	0.01
NaX	0.00	0.03	0.02	0.01	0.03
KX	0.02	0.04	0.05	0.02	0.02
RbX	0.03	0.04	0.06	0.02	0.03
CsX	0.02	0.04	0.05	0.04	0.01
Cu(I)X	0.02	0.07	0.07	0.04	0.00
AgX	0.01	0.05	0.07	0.03	0.01
CaX	0.00	0.05	0.06	0.04	0.03
CuII(X)	-0.01	0.04	0.00	0.01	0.07
PdX	0.00	0.01	0.03	0.03	0.01
PtX	0.00	0.03	0.03	0.03	0.04
FeX	0.01	0.14	0.01	0.06	0.00
CoX	-0.01	0.07	0.07	0.02	0.04
NiX	-0.01	0.09	0.05	0.01	0.05

Table SIII: Intramolecular bonds of the gases during the adsorptions over the different Y and X cation-exchanged faujasites.

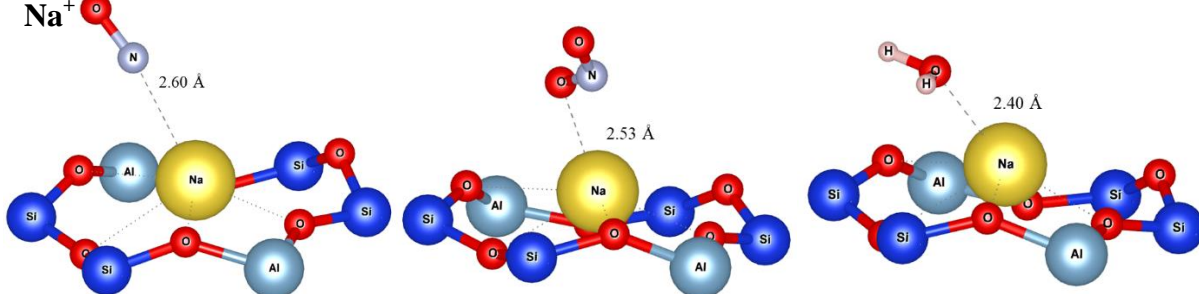
Gas species concerned		NO	NO2	H2O		
Bond		N-O	O1-NO	O2-NO	H1-OH	H2-OH
Initial length (Å)		1.17	1.21	1.21	0.97	0.97
LiY		1.17	1.20	1.22	0.97	0.98
NaY		1.17	1.23	1.20	0.98	0.97
KY		1.17	1.22	1.22	0.99	0.97
RbY		1.17	1.22	1.22	0.98	0.98
CsY		1.17	1.22	1.22	0.98	0.98
Cu(I)Y		1.19	1.29	1.23	1.00	0.97
AgY		1.17	1.22	1.22	0.97	0.99
CaY		1.16	1.26	1.21	0.97	0.98
BaY		1.17	1.23	1.24	0.99	0.99
ZnY		1.17	1.27	1.21	0.98	0.97
Cu(II)Y		1.15	1.23	1.20	0.98	1.00
PdY		1.16	1.21	1.21	0.98	0.98
PtY		1.17	1.21	1.22	0.98	0.98
FeY		1.17	1.17	1.52	0.97	0.98
CoY		1.16	1.16	1.56	0.99	0.98
NiY		1.16	1.24	1.20	0.98	0.98
LiX		1.16	1.23	1.23	0.99	0.98

NaX	1.17	1.24	1.23	0.98	1.00
KX	1.19	1.25	1.26	0.99	0.99
RbX	1.20	1.25	1.27	0.99	1.00
CsX	1.19	1.25	1.26	1.01	0.98
Cu(I)X	1.19	1.28	1.28	1.01	0.97
AgX	1.18	1.26	1.28	1.00	0.98
CaX	1.17	1.26	1.27	1.01	1.00
CuII(X)	1.16	1.25	1.21	0.98	1.04
PdX	1.17	1.22	1.24	1.00	0.98
PtX	1.17	1.24	1.24	1.00	1.01
FeX	1.18	1.35	1.22	1.03	0.97
CoX	1.16	1.28	1.28	0.99	1.01
NiX	1.16	1.30	1.26	0.98	1.02

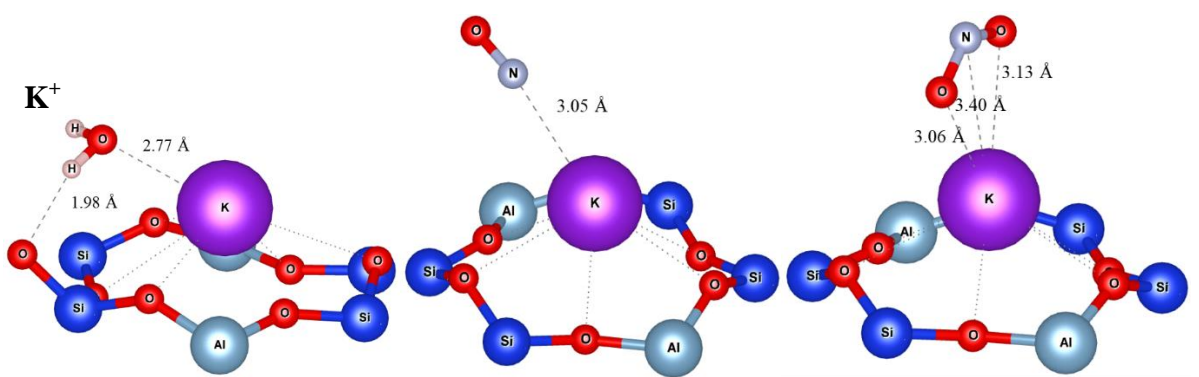
Li⁺



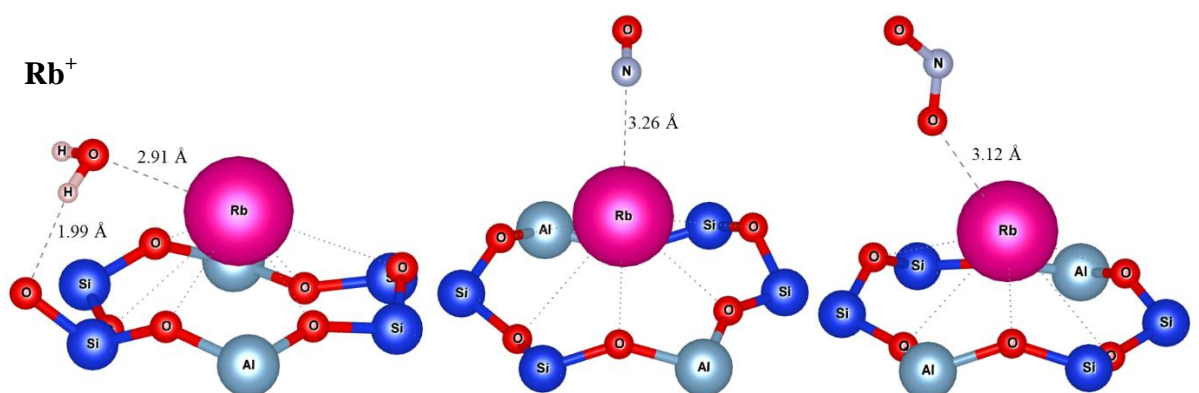
Na⁺



K⁺



Rb⁺



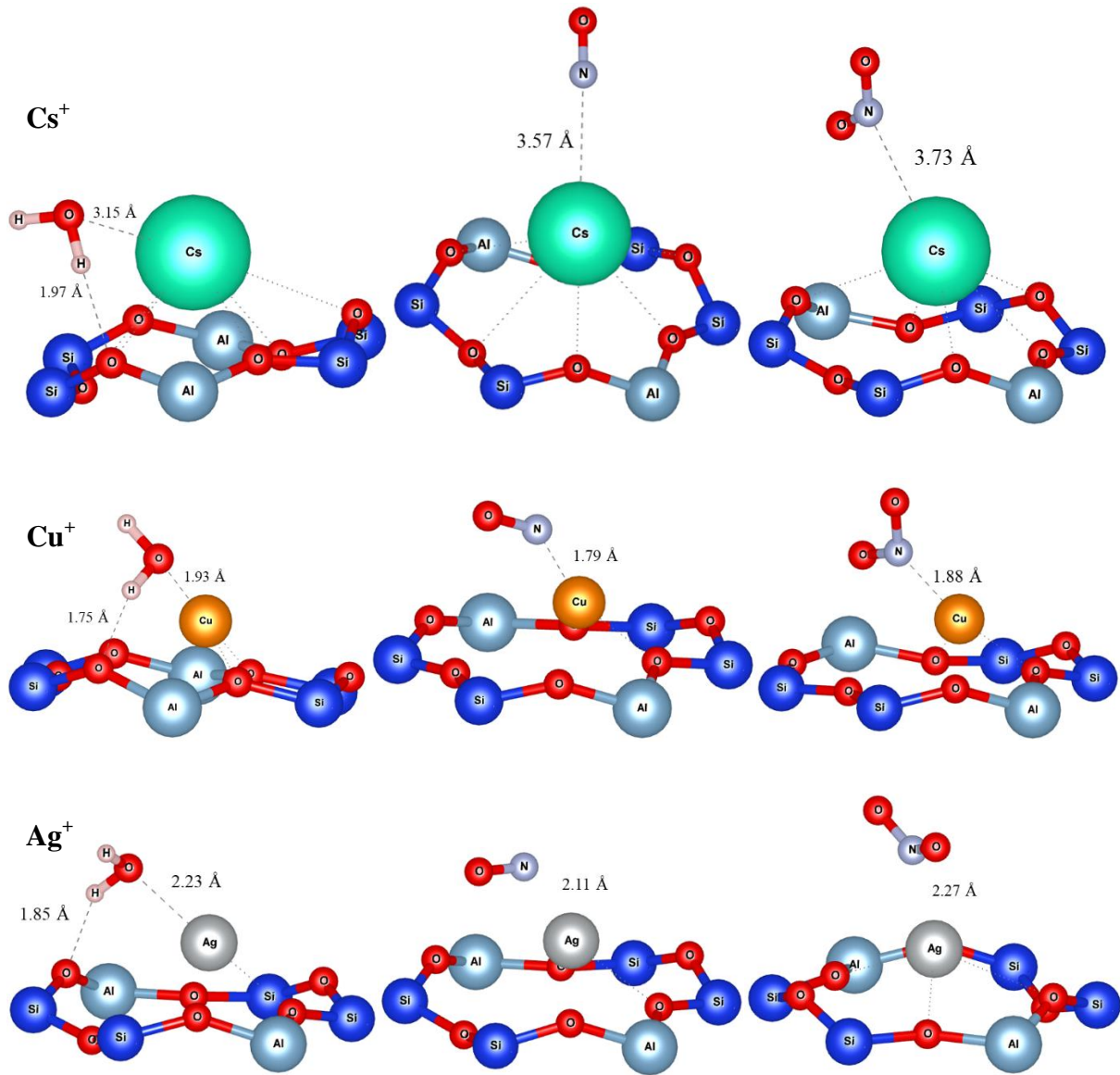
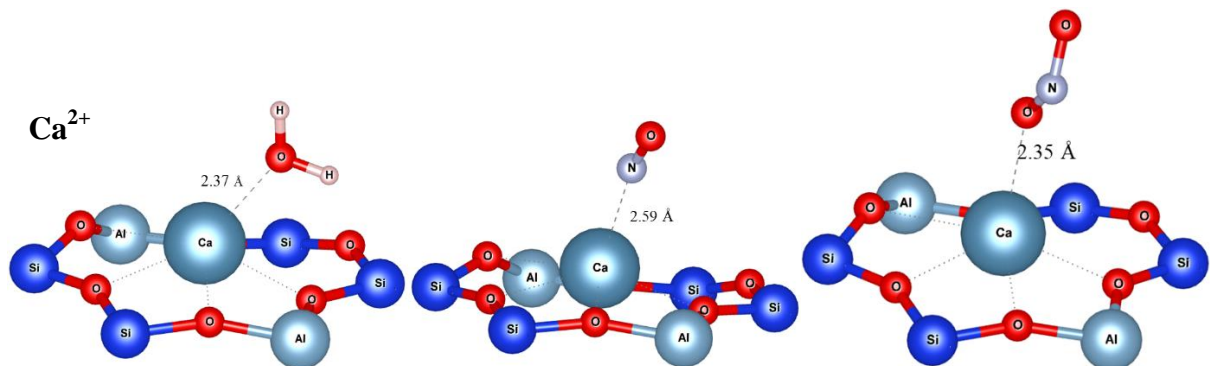
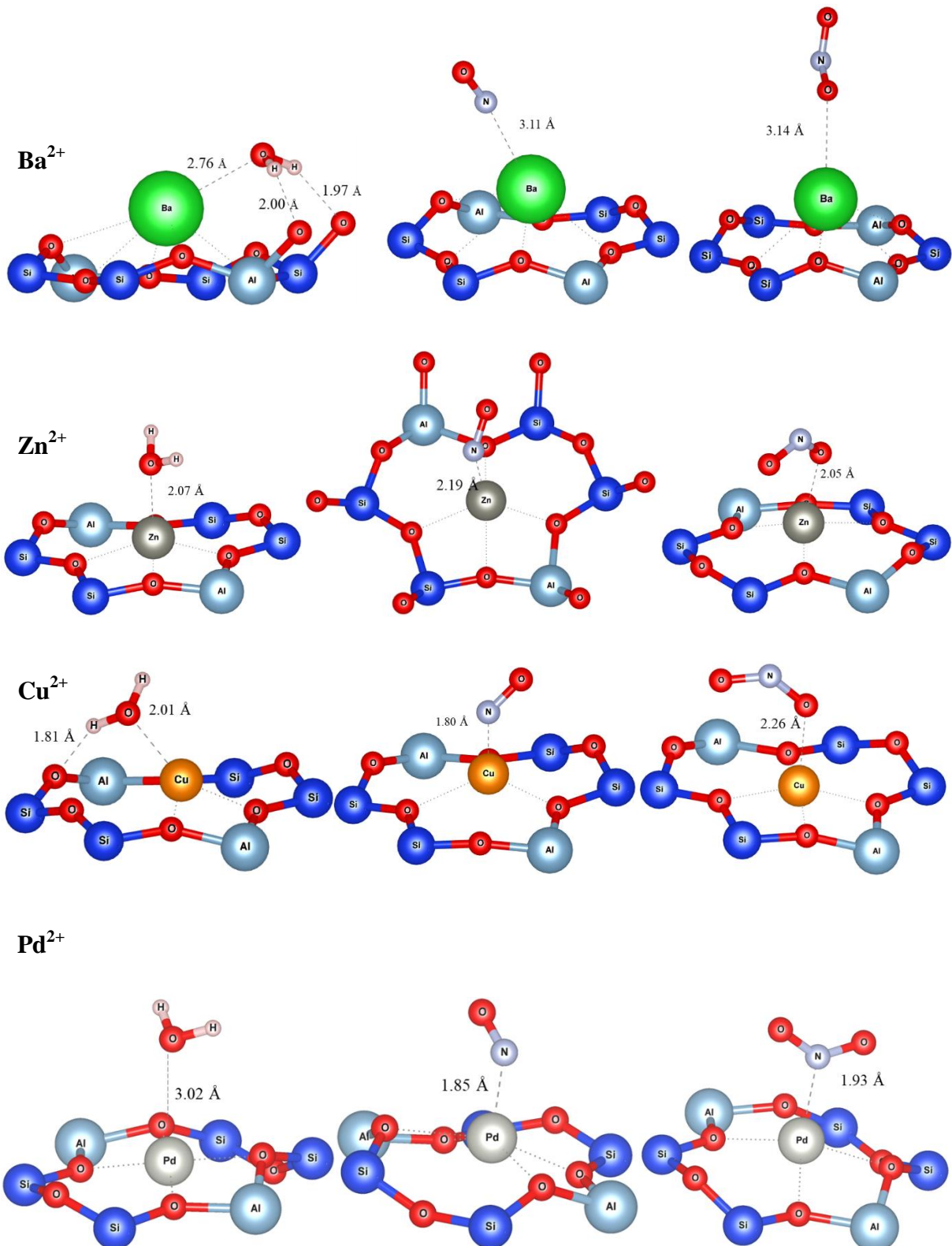


Figure SI: Adsorption modes of the gases (H₂O: left, NO: middle, and NO₂: right) over the different Y monovalent cation-exchanged faujasites.





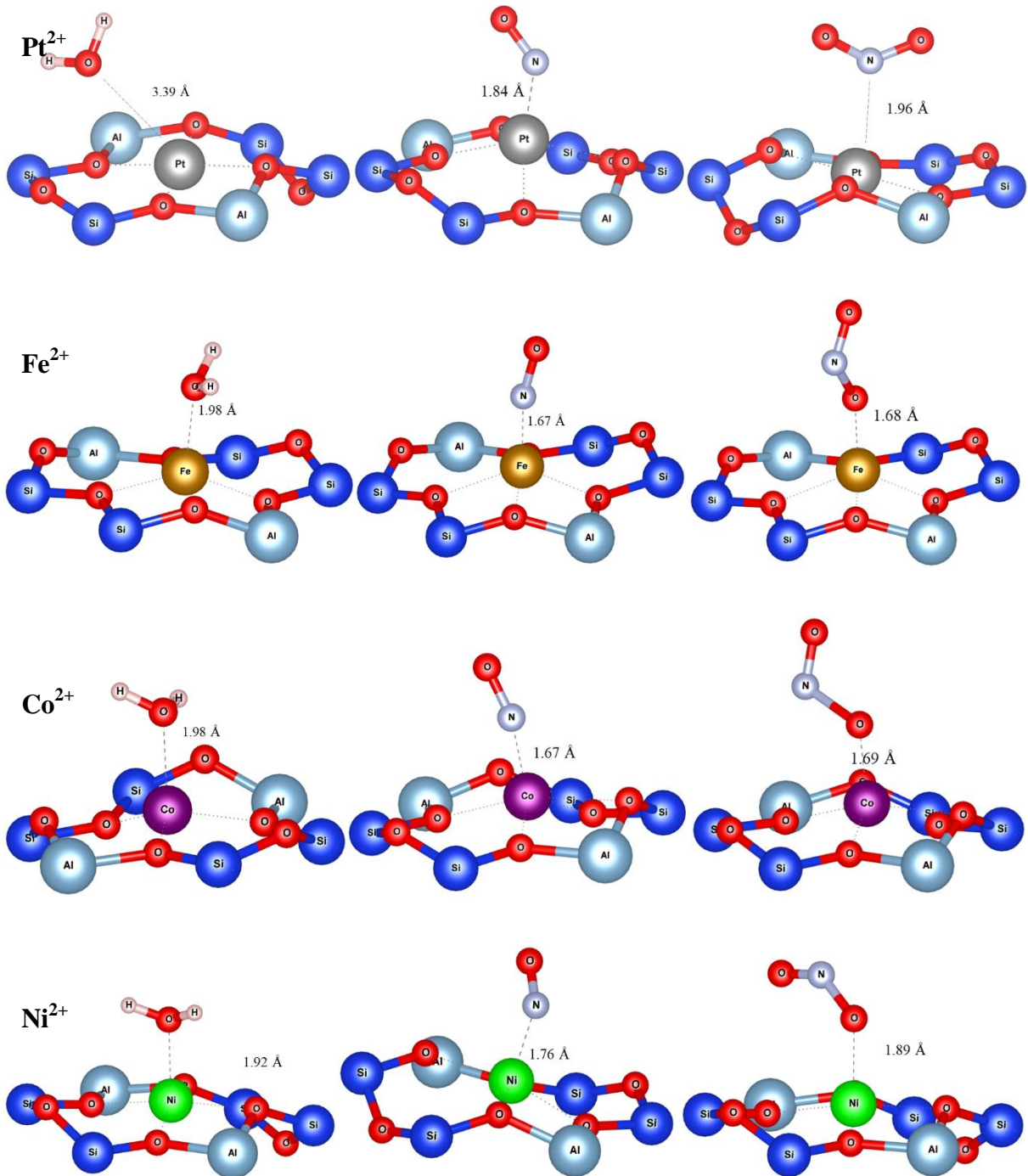
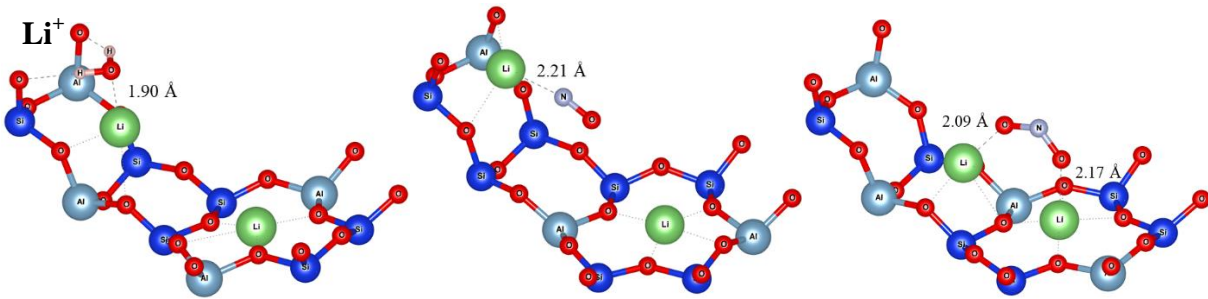
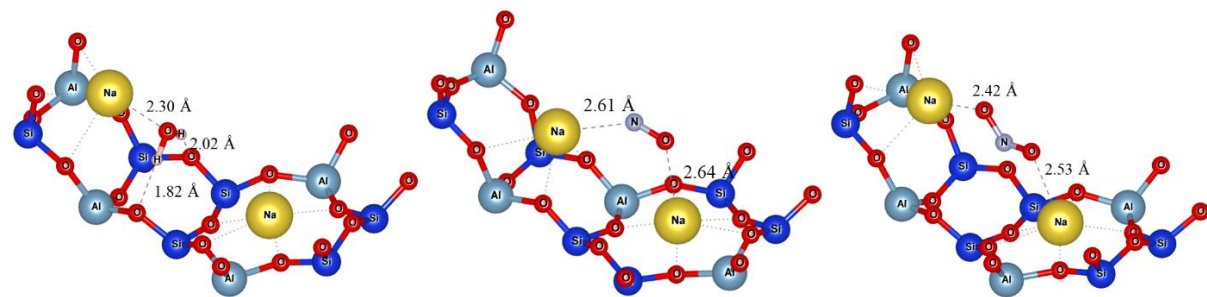


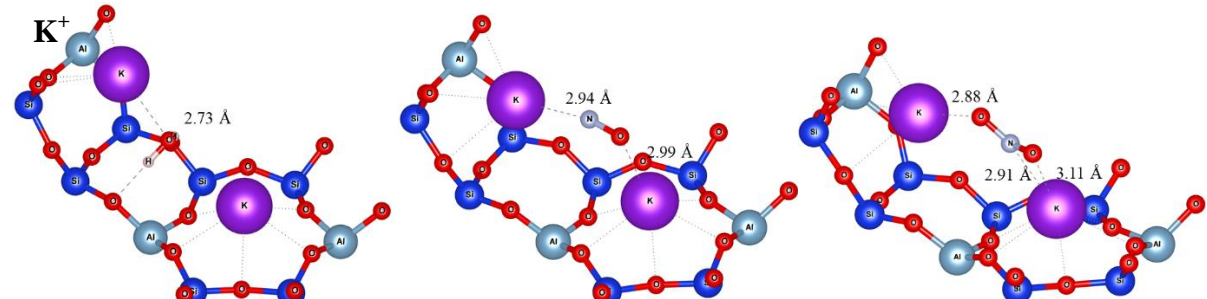
Figure SII: Adsorption modes of the gases (H_2O : left, NO : middle, and NO_2 : right) over the different Y divalent cation-exchanged faujasites.



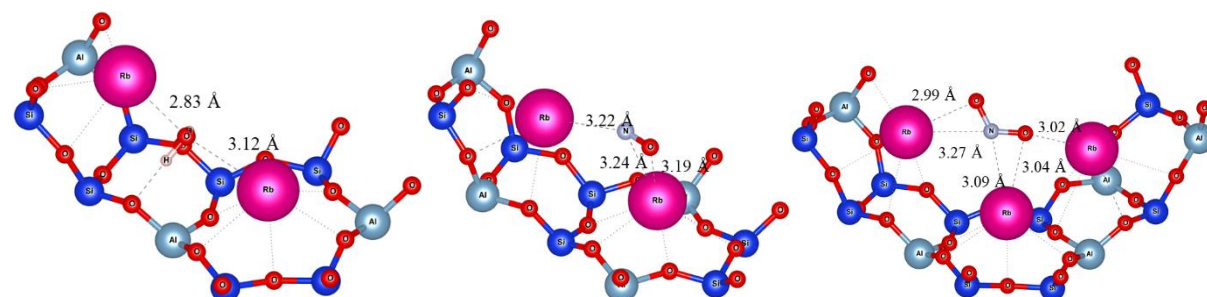
Na⁺



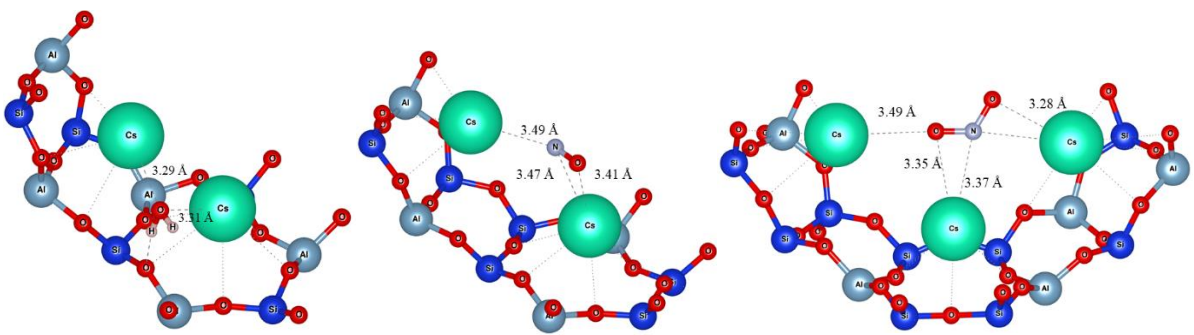
K⁺



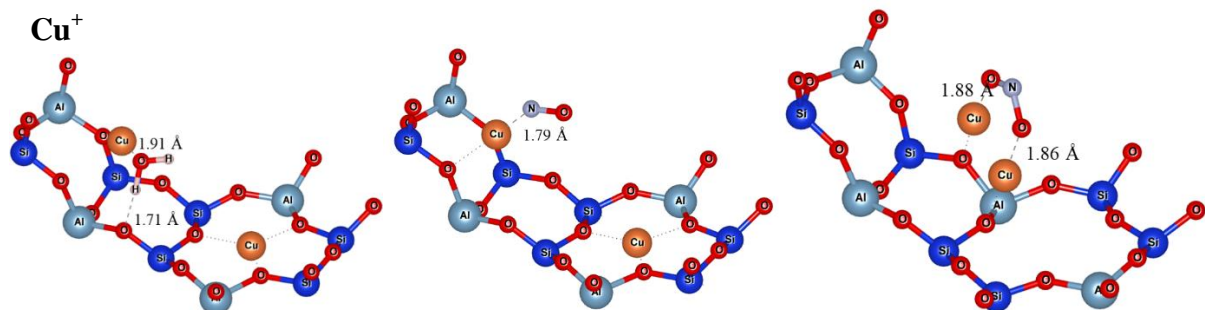
Rb⁺



Cs⁺



Cu^+



Ag^+

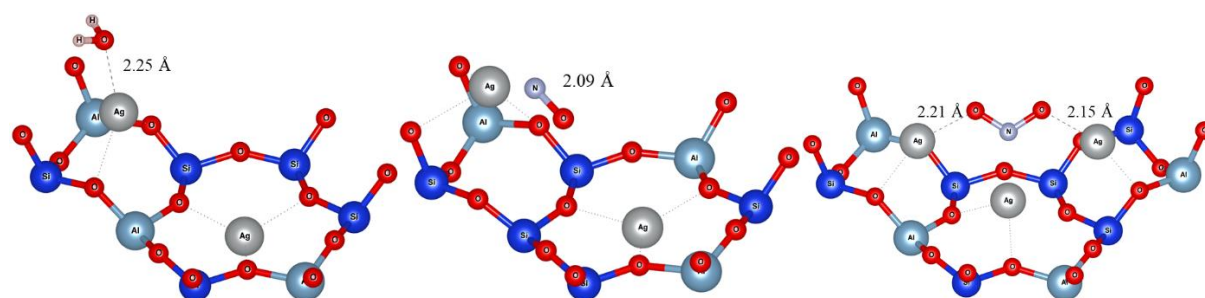
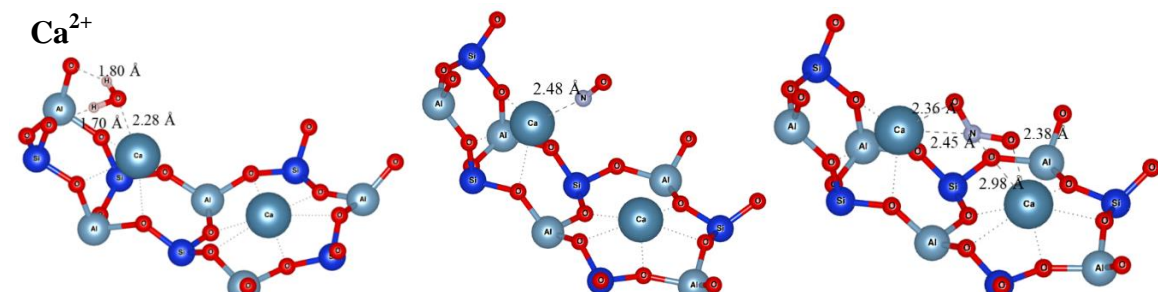
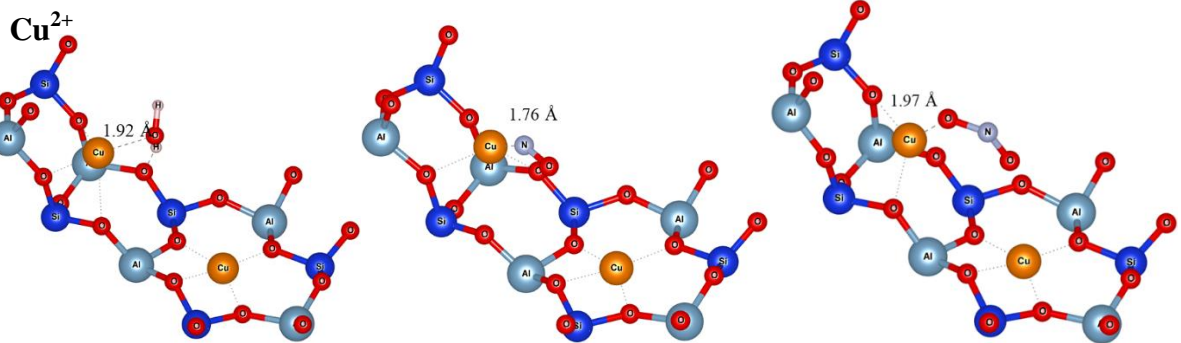


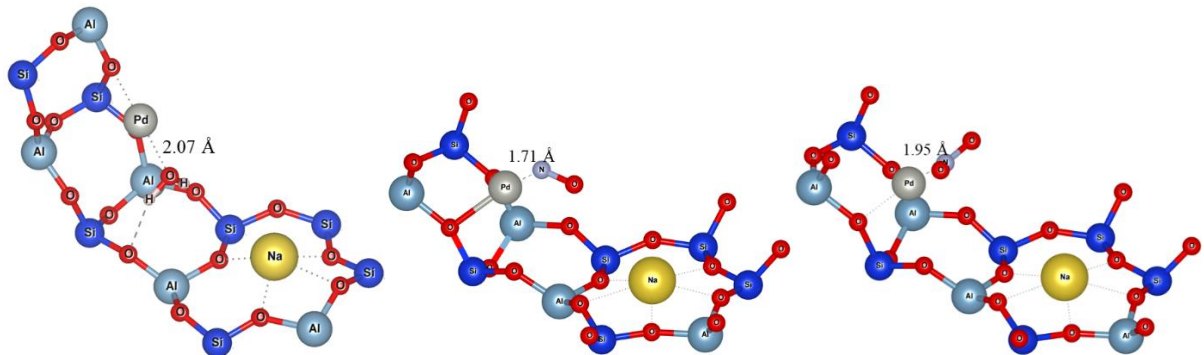
Figure SIII: Adsorption modes of the gases (H_2O : left, NO : middle, and NO_2 : right) over the different X monovalent cation-exchanged faujasites.

Ca^{2+}

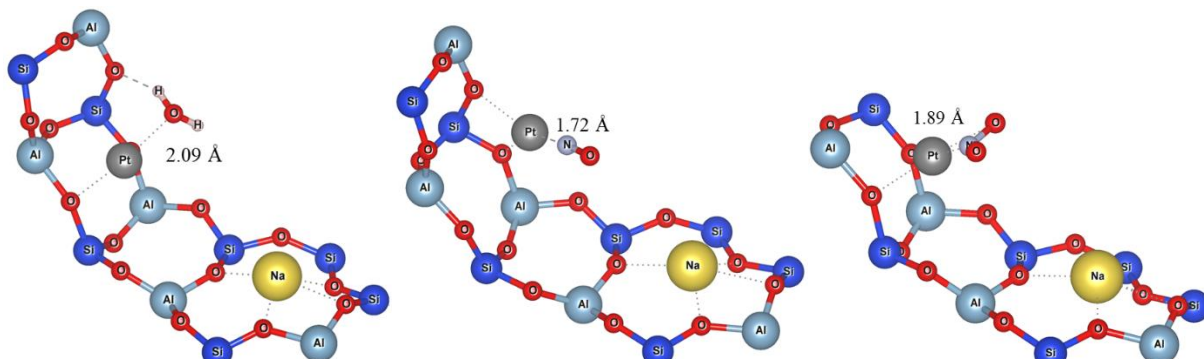




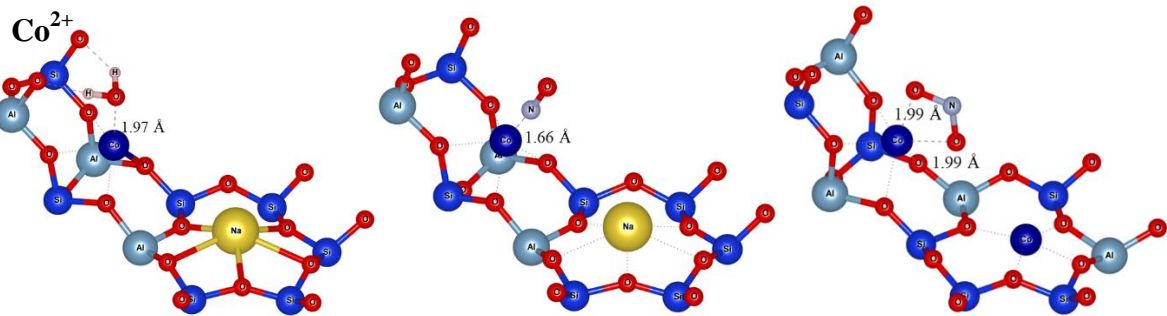
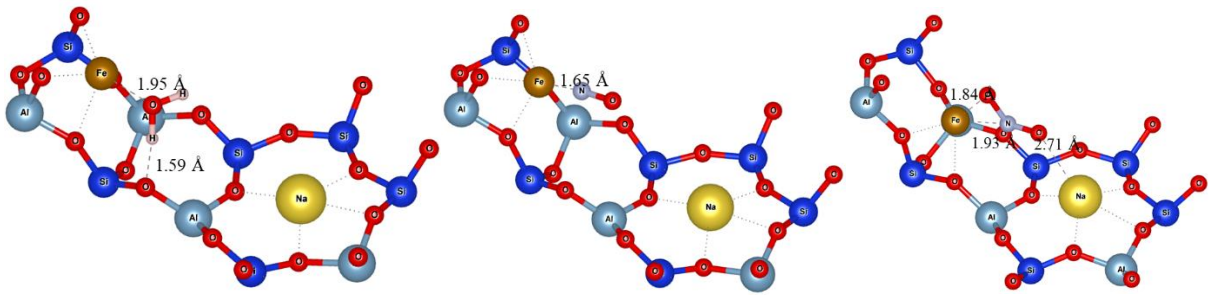
Pd^{2+}



Pt^{2+}



Fe^{2+}



Ni^{2+}

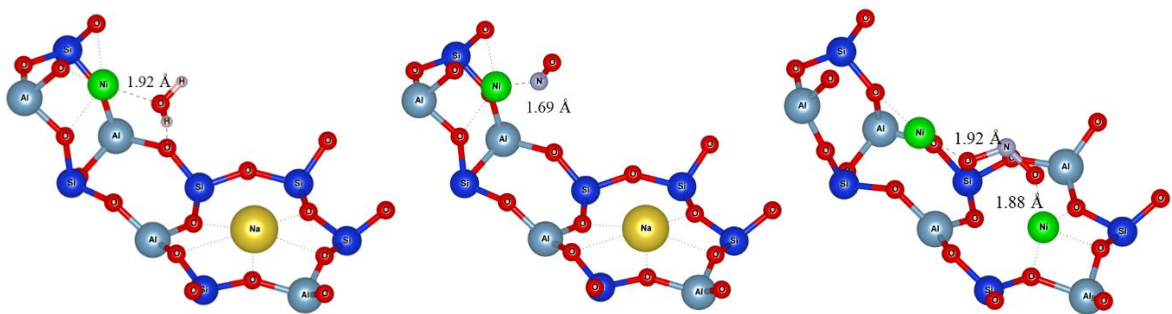


Figure SIV: Adsorption modes of the gases (H_2O : left, NO : middle, and NO_2 : right) over the different X divalent cation-exchanged faujasites.

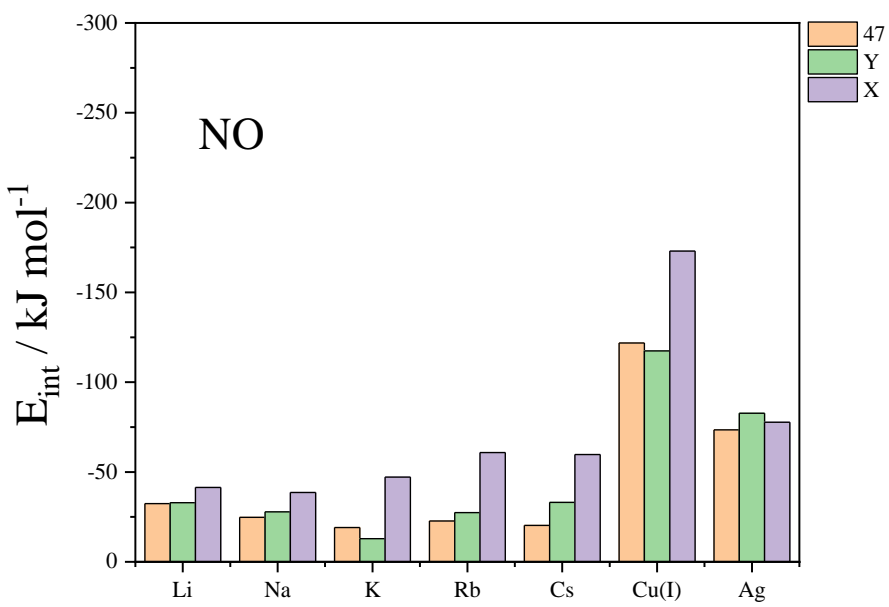


Figure SV: Interaction energies computed at the PBE+D2 level of theory for NO on monovalent cation embedded faujasite with Si/Al = {47, 2.43, 1.4}.

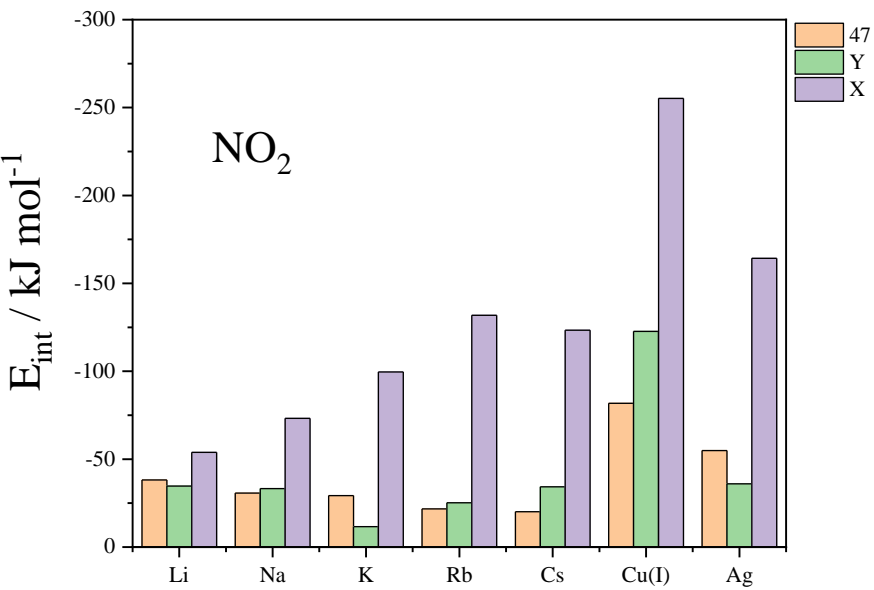


Figure SVI: Interaction energies computed at the PBE+D2 level of theory for NO₂ on monovalent cation embedded faujasite with Si/Al = {47, 2.43, 1.4}.

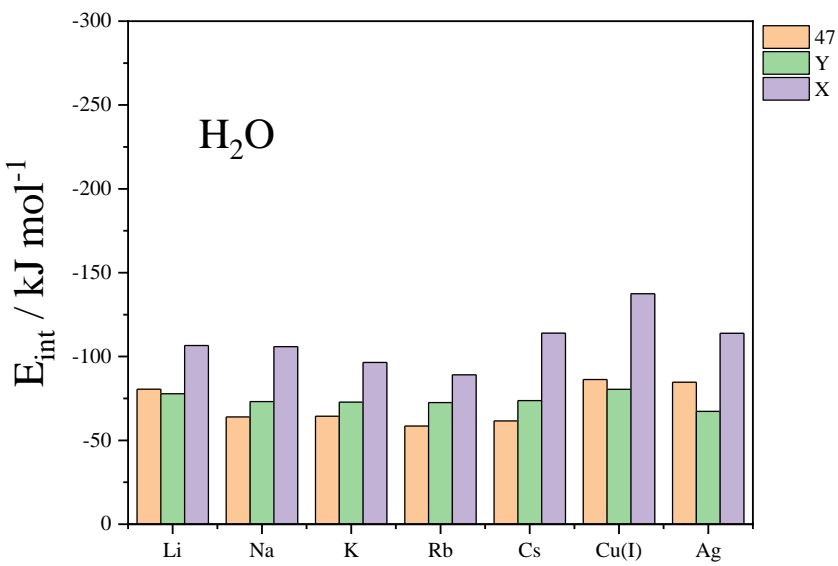


Figure SVII: Interaction energies computed at the PBE+D2 level of theory for H₂O on monovalent cation embedded faujasite with Si/Al = {47, 2.43, 1.4}.

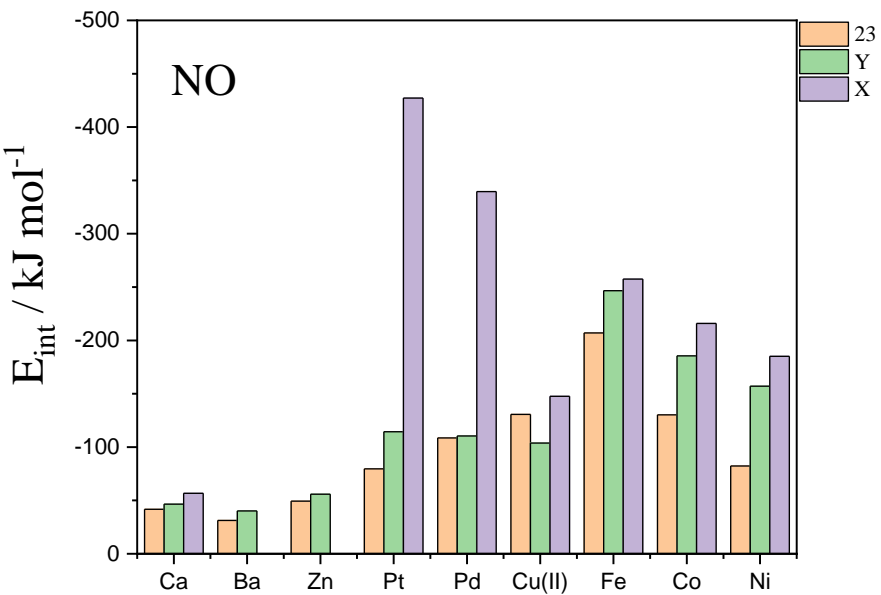


Figure SVIII: Interaction energies computed at the PBE+D2 level of theory for NO on divalent cation embedded faujasite with Si/Al = {23, 2.43, 1.4}.

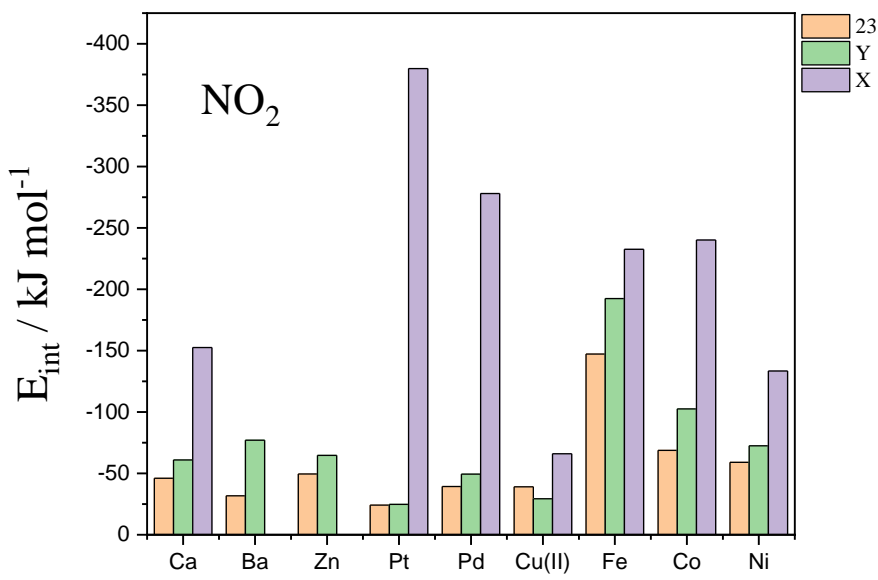


Figure SX: Interaction energies computed at the PBE+D2 level of theory for H_2O on divalent cation embedded faujasite with $\text{Si}/\text{Al} = \{23, 2.43, 1.4\}$.

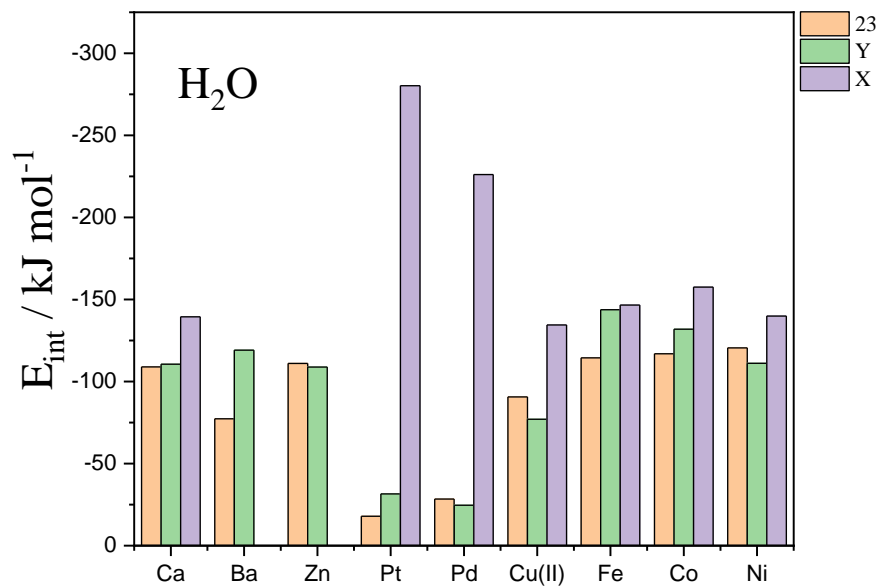


Figure SX: Interaction energies computed at the PBE+D2 level of theory for H_2O on divalent cation embedded faujasite with $\text{Si}/\text{Al} = \{23, 2.43, 1.4\}$.

Table SIV: The induced intramolecular bond changes of NO₂ due to its adsorption on Cu(I)Y, PdY, PtY, FeY, CoY and NiY (Si/Al = 2.43), are presented. The configurations considered are 1: through N (M – N – O₂), 2: through O1 while N and O2 are ordered perpendicularly to the 6MR (M – O1 – N | O₂) and 3: through O1 while N and O2 are ordered parallelly to the 6MR (M – O1 – N – O₂). The values in brackets correspond to the stretching with respect to the initial bond length in percentages. In the second line we also include the interaction energy that complemented these configuration modes.

Gas species concerned	M – N – O ₂		M – O1 – N – O ₂		M – O1 – N O ₂		
	Bond	O1-NO	O2-NO	O1-NO	O2-NO	O1-NO	O2-NO
Cu(I)Y (Å)		0.08 (7%) (-122.7)	0.02 (2%)	0.08 (7%) (-88.4)	0.01 (1%)	0.10 (8%) (-96.1)	0.01 (1%)
PdY (Å)		0.01 (-120.8)	0.01	Not Stable	Not Stable	Not Stable	Not Stable
PtY (Å)		0.01 (-137.6)	0.01	Not Stable	Not Stable	Not Stable	Not Stable
FeY (Å)		0.11 (9%) (-173.6)	-0.01 (-1%)	0.31 (26%) (-192.3)	-0.04 (-3%)	0.31 (26%) (-192.4)	-0.04 (-3%)
CoY (Å)		0.02 (-94.7)	0.02	0.07 (-94.7)	0.00	0.35 (-102.6)	-0.05
NiY (Å)		0.01 (-71.4)	0.01	0.03 (-72.5)	-0.01	0.08 (-64.8)	-0.01

Table SV: The intramolecular bonds of NO₂ after its adsorption on Cu(I)Y, PdY, PtY, FeY, CoY and NiY (Si/Al = 2.43), are presented. The configurations considered are 1: through N (M – N – O₂), 2: through O₁ while N and O₂ are ordered perpendicularly to the 6MR (M – O₁ – N | O₂) and 3: through O₁ while N and O₂ are ordered parallelly to the 6MR (M – O₁ – N – O₂). The values in brackets correspond to the stretching with respect to the initial bond length in percentages.

Gas species concerned	M – N – O ₂		M – O ₁ – N – O ₂		M – O ₁ – N O ₂	
	Bond	O1-NO	O2-NO	O1-NO	O2-NO	O1-NO
Cu(I)Y (Å)	1.28 (7%)	1.23 (2%)	1.29	1.22	1.31	1.22
PdY (Å)	1.22	1.22	Not Stable	Not Stable	Not Stable	Not Stable
PtY (Å)	1.22	1.22	Not Stable	Not Stable	Not Stable	Not Stable
FeY (Å)	1.32	1.20	1.52	1.17	1.52 (26%)	1.17 (-3%)
CoY (Å)	1.23	1.23	1.28	1.21	1.56	1.16
NiY (Å)	1.22	1.22	1.24	1.20	1.29	1.20

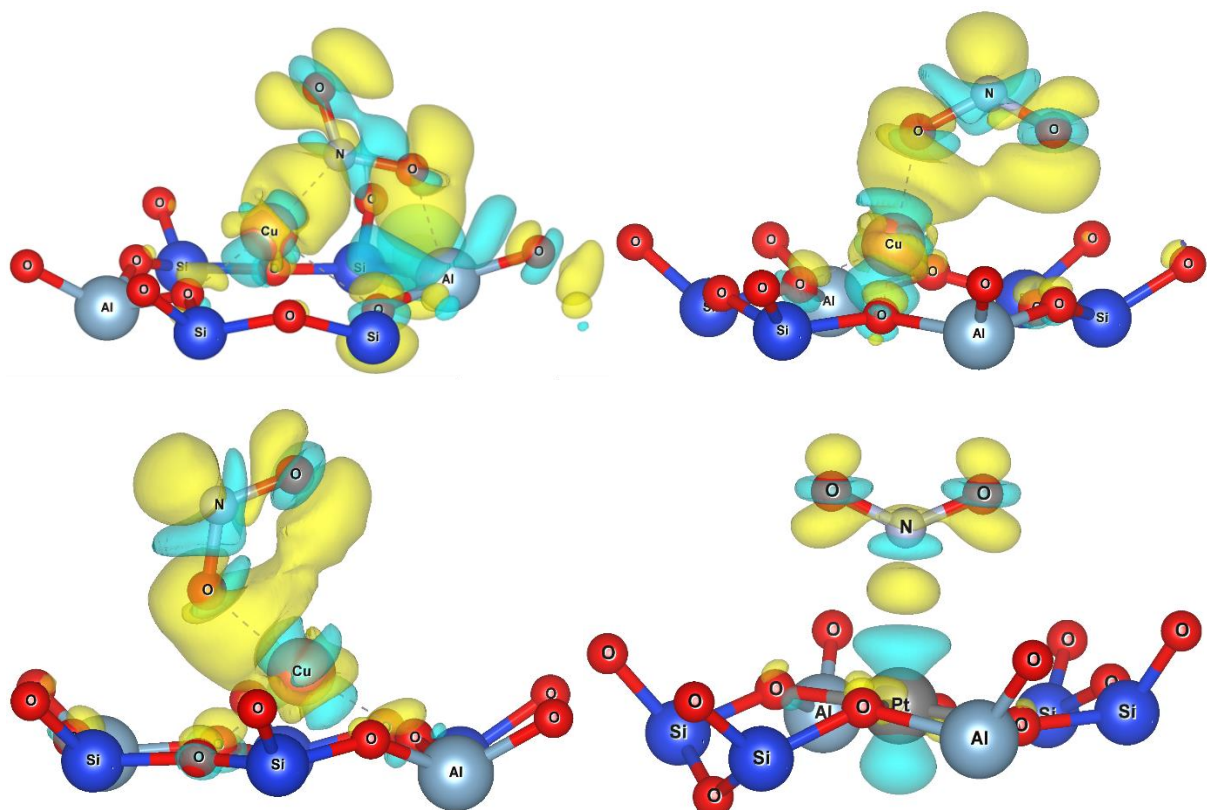
Table SVI: Bader charge differences due to adsorptions of NO₂ calculated for the systems Cu(I)Y, PdY, PtY, FeY, CoY and NiY. The configurations considered are 1: through N (M – N – O₂), 2: through O₁ while N and O₂ are ordered perpendicularly to the 6MR (M – O₁ – N | O₂) and 3: through O₁ while N and O₂ are ordered parallelly to the 6MR (M – O₁ – N – O₂).

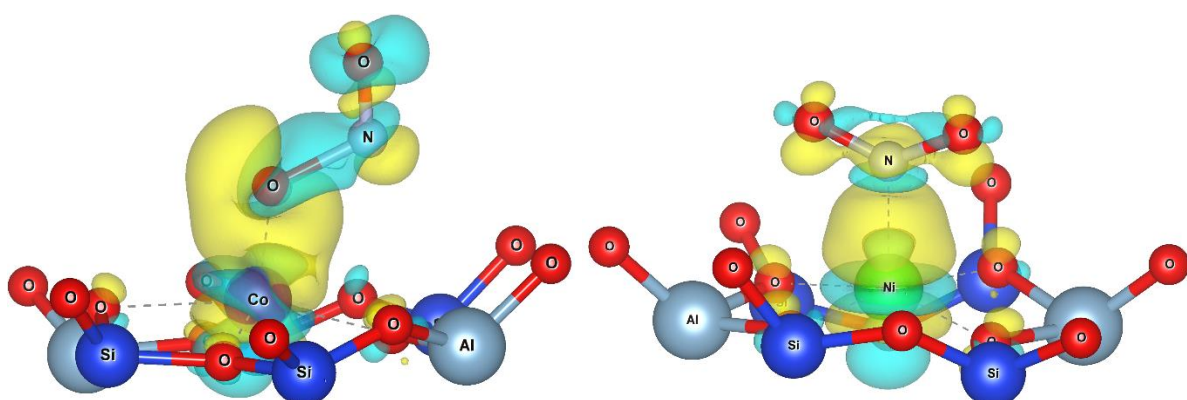
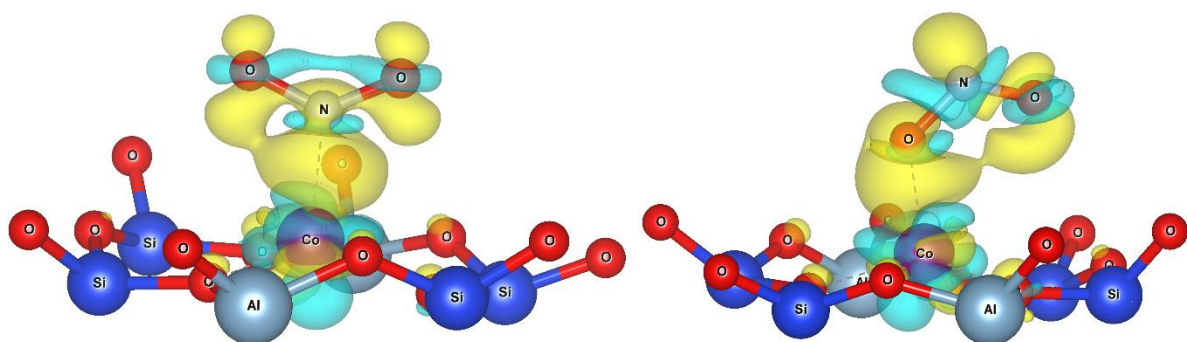
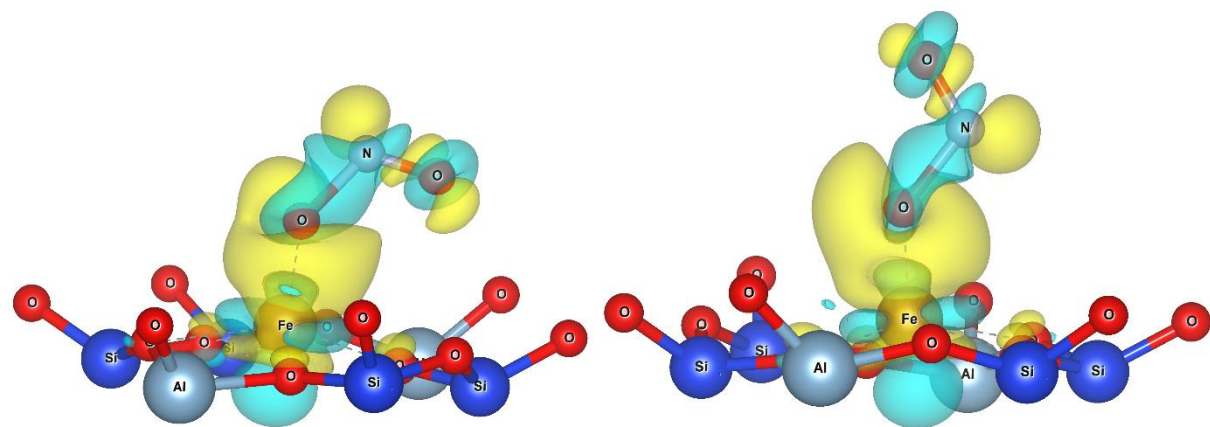
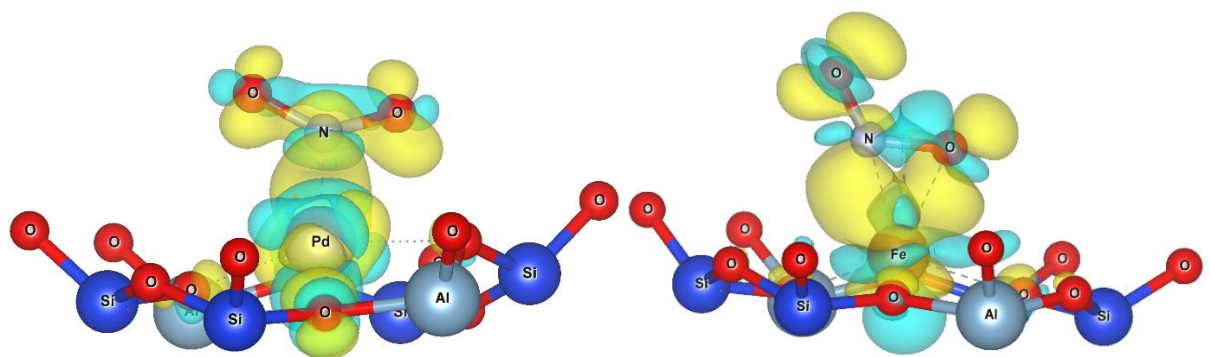
Cation	config	Atom	Charge Difference
Cu(I)	– N – O ₂	O1	-0.156
		O2	-0.134
		N	-0.204
	– O ₁ – N O ₂	Cu(I)	0.102
		O1	-0.292
		O2	-0.137
		N	-0.075
		Cu(I)	0.110
		O1	-0.254
		O2	-0.179
		N	-0.017
		Cu(I)	0.159
Pd	– N – O ₂	O1	-0.010
		O2	-0.036
		N	-0.087
		Pd	0.083
	– O ₁ – N O ₂	O1	Not Stable
		O2	
		N	
		Pd	
		O1	Not Stable
		O2	
		N	
		Pd	
Pt	– N – O ₂	O1	-0.044
		O2	0.001
		N	-0.108
		Pt	0.113
	– O ₁ – N O ₂	O1	Not Stable
		O2	
		N	
		Pt	

	$- \text{O}1 - \text{N} - \text{O}2$	O1 O2 N Pt	Not Stable
Fe	$- \text{N} - \text{O}_2$	O1 O2 N Fe	-0.218 -0.048 -0.156 0.196
	$- \text{O}1 - \text{N} \text{O}2$	O1 O2 N Fe	-0.370 -0.021 0.040 0.233
	$- \text{O}1 - \text{N} - \text{O}2$	O1 O2 N Fe	-0.369 -0.050 0.055 0.227
Co	$- \text{N} - \text{O}_2$	O1 O2 N Co	-0.045 -0.034 -0.149 0.038
	$- \text{O}1 - \text{N} \text{O}2$	O1 O2 N Co	-0.334 0.017 0.086 0.165
	$- \text{O}1 - \text{N} - \text{O}2$	O1 O2 N Co	-0.212 -0.046 -0.007 0.096
Ni	$- \text{N} - \text{O}_2$	O1 O2 N Ni	0.010 0.008 -0.097 0.007
	$- \text{O}1 - \text{N} \text{O}2$	O1 O2 N Ni	-0.158 0.017 0.031 0.121
	$- \text{O}1 - \text{N} - \text{O}2$	O1 O2 N Ni	-0.085 0.055 0.024 0.053

Table SVII Magnetic moments of the zeolites before and after the adsorption

System	Before	NO	N-O2	O1-N-O2	O1-N O2	H2O
Cu(I)Y	0.00	1.00	0.63	0.52	0.53	0.00
PdY	0.00	0.00	0.00	Not Stable	Not Stable	0.00
PtY	0.00	0.00	0.97	Not Stable	Not Stable	0.00
FeY	24.00 (6*4)	23.00	25.00	25.00	25.00	24.00
CoY	17.97 (6*3)	16.95	17.94	18.00	18.92	17.97
NiY	11.7 (6*2)	10.74	11.43	12.70	11.04	11.76





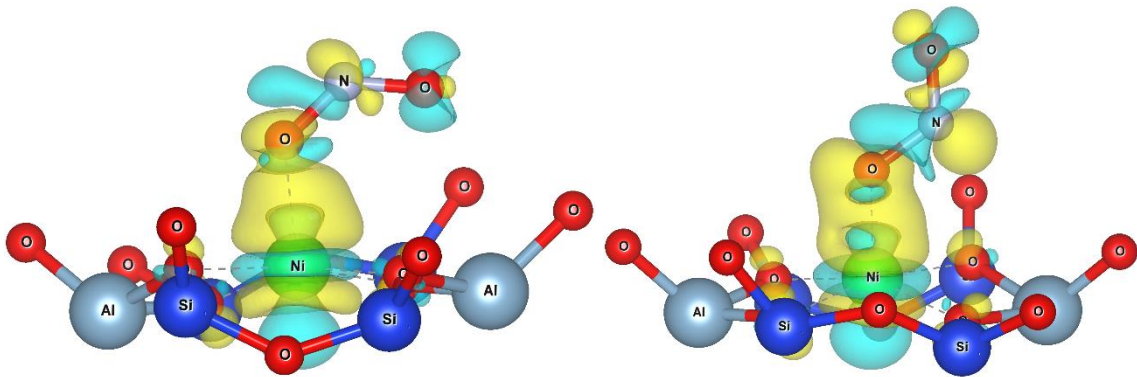


Figure SXI: Charge density differences that occurred during the adsorption NO_2 on Cu(I)Y, PtY, PdY, FeY, CoY, NiY through 3 different modes: 1: through N ($\text{M} - \text{N} - \text{O}_2$), 2: through O1 while N and O2 are ordered perpendicularly to the 6MR ($\text{M} - \text{O}_1 - \text{N} | \text{O}_2$) and 3: through O1 while N and O2 are ordered parallelly to the 6MR ($\text{M} - \text{O}_1 - \text{N} - \text{O}_2$). The isosurfaces have a density $0.002 \text{ } e/\text{a}_0^3$.

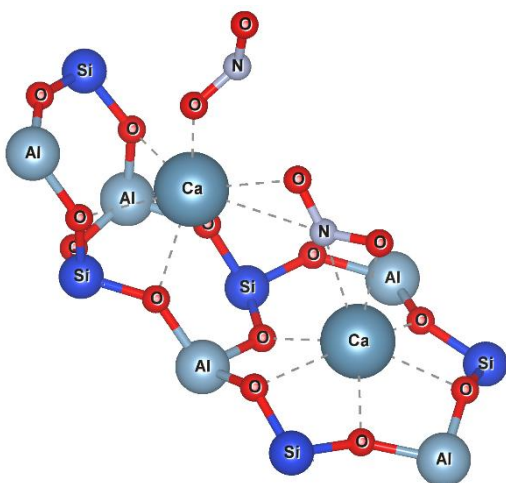
To investigate the potential effects of increased NO_2 coverage on the possibility of cross-adsorption in X zeolite, we performed a series of geometry optimization calculations. Specifically, we began with relaxed NO_2 cross-adsorption geometries and then introduced a second NO_2 molecule in close proximity to one of the two-adsorption sites. We then evaluated whether the second NO_2 molecule was able to adsorb and whether it obstructed the cross-adsorption of the first NO_2 molecule. We carried out these calculations for X zeolite exchanged with Ca, Fe, and Ni. The resulting adsorption modes for the two NO_2 molecules are displayed in Figure SXII.

In the case of Ca, we study the cross adsorption between two Ca cations, representing alkali earths. When the second NO_2 was placed close to site III', it adsorbed successfully, while the first NO_2 molecule stayed cross-adsorbed. When the second NO_2 was placed close to site II, its adsorption was prevented by steric affects, between the two NO_2 molecules. An

overall interaction energy of -192.9 kJ/mol is associated with the simultaneous adsorption of the two gases.

FeX cross-adsorption occurred between one Fe and one Na cation, namely between a transition metal in site III' and an alkali metal in site II. The presence of a second NO₂ gas did not prevent the cross-adsorption of the first. Two configurations were obtained dependent on whether the second NO₂ was adsorbed on a) site III' Fe or, b) on site II Na. These two adsorption configurations are associated with interaction energies of -333.1 and -266.5 kJ/mol, respectively.

In the case of Ni, we studied the cross adsorption between two Ni cations, namely between two transition metals. The first NO₂ molecule stayed cross-adsorbed, when the second was placed near site II or site III'. The second, adsorbed by both site II and site III', one at a time, giving rise to interaction energies of -138.3 and 230.0 kJ/mol, respectively.



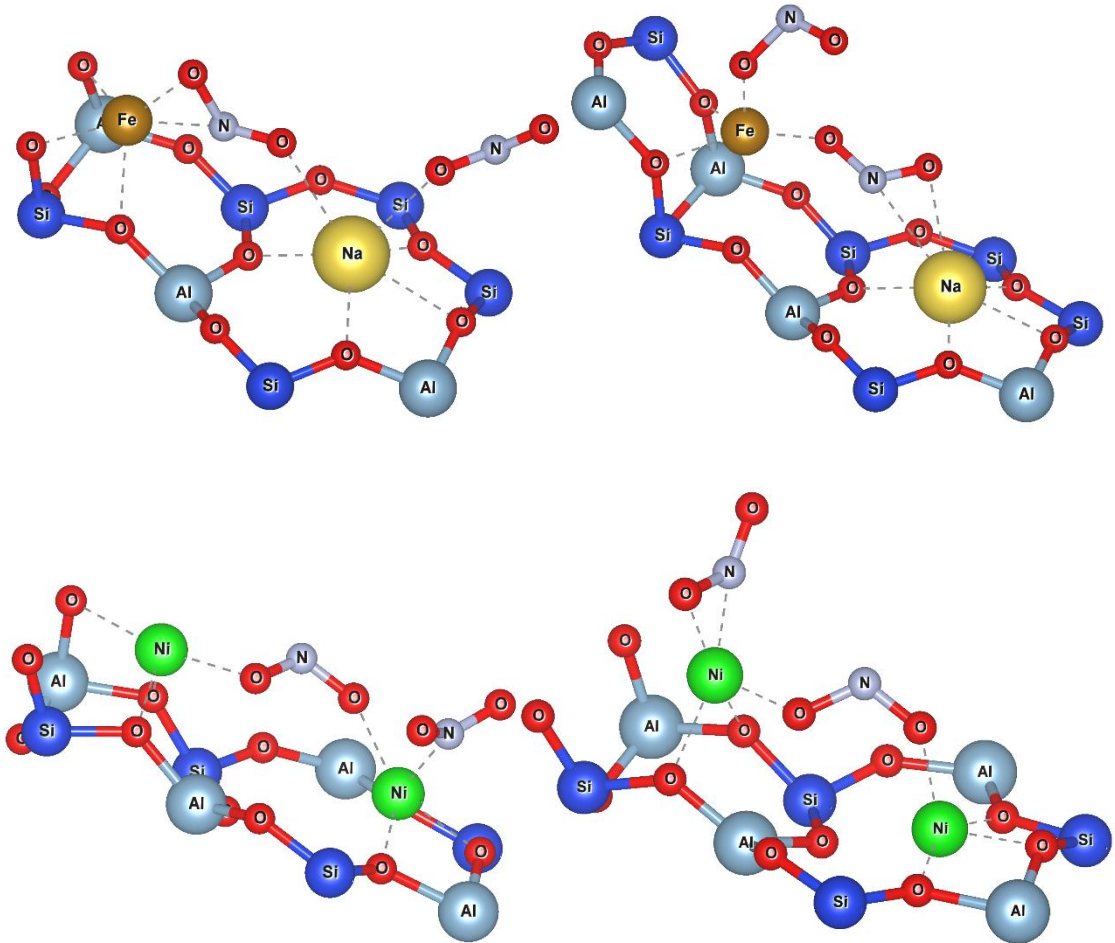


Figure SXII: Adsorption of 2 NO₂ molecules on the same sites of X zeolite. One NO₂ molecule stays always cross-adsorbed, while the second potentially adsorbs, by either a site II or site III' cation.